Determination of Fluid Flow Mechanisms in Berea Using Mercury Porosimetry and A Stochastic Model to Relate These Mechanisms to Oil Recovery

SCA Number 9123

by

Dr. Robert W. Watson

The Pennsylvania State University

Fathi H. Boukadi

The Pennsylvania State University

This work is part of on-going research aimed at correlating rock skeletal properties to oil recovery from sandstone, limestone and dolomite cores and incorporating these properties into a stochastic model for predicting oil recovery. As such, this report is divided into the analyses and interpretation of experimental data collected from core floods and correlated against measurements of wettability, tortuosity, pore entry diameter, surface area and pore length and the presentation of a stochastic model based on data obtained from these laboratory experiments which relates rock skeletal properties to oil recovery.

Analyses suggest that capillary pressure curve shapes and mercury incremental intrusion volume plots are useful in describing pore-size distribution in porous media. Further analysis shows that snap-off and bypassing mechanisms are related to the pore aspect ratio(ratio of pore-body to pore-throat) and to pore connectivity. Mercury trapping is pronounced in Berea cores where cul-de-sac configurations are abundant. Cul-de-sacs with significant pore aspect ratios are characterized by a high degree of trapping. Moreover, limited pore connectivity enhances trapping and mercury isolation as discontinuous blobs of mercury are difficult to recover following the intrusion-extrusion cycle.

In a Berea core, a strongly water-wet rock, the mercury-air system is best suited to represent an oil-brine system. Extensive experiments using 524 core plugs revealed that mercury recovery efficiency is related to rock porosity, pore hydraulic diameter and surface area available to the non-wetting phase. Analyses show that under capillary force dominance, mercury recovery efficiency is high for the tighter cores which have a small pore-entry diameter and a large rock surface area.

The results of the core analyses have been incorporated into a stochastic model. This model, based on reservoir architecture, can be used to predict reservoir performance and consequently oil recovery. The skeletal properties contained in the model will include: hydraulic diameter, rock surface area, pore-size distribution, wettability, tortuosity and porosity.

INTRODUCTION

The mechanisms of oil dispacement by waterflooding were investigated using radial Berea sandstone cores. Furthermore, a frontal advance rate of one foot/day was selected to simulate fluid flow mechanisms in strongly water-wet systems where capillary forces are the predominant driving mechanisms. The ratio of viscous to capillary to forces for this system was calculated to be 1.344×10^{-7}. The oil produced was shown to be dependent to a large extent on the size, shape, arrangement and distribution of pores, rock porosity, surface area, wettability and tortuosity of the connecting throat passages.

Pore-size distribution, pore-entry diameter and rock surface area were determined using mercury porosimetry analysis. Mercury porosimetry analysis is used to investigate the mechanisms of non-wetting phase trapping and the influence of rock microscopic skeletal properties on oil recovery. Pickell, Swanson and Hickman (1) found that air-mercury capillary pressure data adequately describe the distribution of fluids in a water-oil system when strong wetting conditions prevail. They also indicated that such data is extremely useful in the study of pore structure and the degree of fluid interconnection at various saturations. Furthermore, Purcell (2) used air-mercury capillary injection curves to characterize the drainage curve and the rock pore structure.

Wettability indices were determined using the Amott-Harvey method. Chatzis et al. (3) indicated that under water-wet conditions, residual oil saturation is affected by particle size, particle size-distribution, macroscopic and microscopic heterogeneities, microscopic dimensions such as the ratio of pore-body to pore-throat size, and the pore-to-pore coordination number.

Pickell, Swanson and Hickman (1) suggested that the degree of wettability of a reservoir rock is an important factor in waterflood or imbibition experiments. Additionally, they indicated that in the case of water-wet rock and reasonably low oil/water viscosity ratio, capillary forces affect the displacement of oil by brine in two ways. On the microscopic scale, capillary forces control the

distribution of fluids in the pore spaces at all saturations. On the macroscopic scale, differences in capillary forces at the flooding front result in the brine flowing into regions of high oil saturation. Therefore, capillary forces tend to erode fingering and bypassed oil patches and bring about a diffuse saturation gradient at the front. The slope of the front with respect to the horizontal will depend upon the rate of the frontal advance and the mobility characteristics. Furthermore, Kimbler and Caudle (4) indicated that for water-wet rocks, capillary forces control the distribution of fluids and viscous forces by contrast have a minimal influence on residual oil saturation and on oil recovery by waterflooding. It should follow therefore that if the ultimate oil recovery is controlled by pore geometry, a unique residual non-wetting phase saturation should exist for a given initial non-wetting phase saturation.

Engelberts and Perkins (5) and Craig (6) have reported that ultimate oil recovery realized in laboratory water-drive experiments conducted in water-wet rocks differ from that realized in reservoirs at field rates. Furthermore, evidence was provided to show that fluid distribution in a porous medium is a function of pore-size distribution, pore configurations, interfacial properties and previous saturation history. Laboratory measurements of air-mercury capillary pressure hysteresis was proposed as a useful technique for predicting fluid distribution for water-wet conditions. Residual non-wetting phase saturations were shown to be a function of pore geometry and initial saturation.

RESULTS AND DISCUSSION

Waterflood Results

As previously noted by Watson and Boukadi (7), there was a tendency for residual oil to increase as the initial oil saturation increased in the waterflooded Berea sandstone rocks. Our findings are in agreement with Pickell et al. (1), Wardlaw et al. (8), Chatzis and Dullien (9), and Wyman (10). Willhite (11) stated that for waterflooding experiments conducted in strongly water-wet rocks (such as Berea sandstone at a Darcy flow rate of 1 foot/day), capillary forces strongly affected the distribution of fluids. The viscous forces, however, had only a minimal influence on residual oil saturation. In this study, the ratio of viscous to capillary forces was calculated to be 1.344×10^{-7}. Therefore the residual oil saturation resulting from waterflooding was influenced by capillary forces only. The effect of the initial and residual oil saturations on oil recovery by waterflooding was taken into account by including these variables in the stochastic model.

Moreover, in the case of a reservoir acting under capillary pressure dominance, tortuosity, τ, of the connecting throat passages was shown by Watson and Boukadi (7) to affect the outcome of oil recovery by waterflooding. To reduce the margin of error and improve the model prediction capabilities, tortuosity, a reservoir architecture component, was incorporated into the stochastic model.

Wettability Results

Relative wettability was determined using the Amott-Harvey method. As described in the previous work by Watson and Boukadi (7), wettability indices varied from a minimum value of +0.45 to a maximum value of +1.00 or absolute water wettability. It was concluded that Berea sandstone wettability was described as "dalmatian" with some parts of the rock being water-wet and others being oil-wet. Furthermore, wettability is "dalmatian" mainly because of the occurence of shaley streaks in the Berea sandstone cores tested. The mean wettability was found to be functionally related to the amount of hydrophobic or hydrophilic surface area present in each core sample.

The behavior of capillary pressure is critical in secondary recovery processes where the average displacement frontal advance rate is low. Capillary pressure is a function of the contact angle, which in turn, is a function of the wetting properties of the fluids and rock surfaces. In designing the stochastic model, one of the independent variables incorporated into the model to account for capillary pressure was the relative wettability. Our analysis indicated that oil recovery by waterflooding is

related to the degree of water-wetness. Waterflood experiments conducted in strongly water-wet Berea core resulted in a higher oil recovery as compared to a less water-wet medium.

Mercury Porosimetry Results

Pore-entry diameter and rock surface area are two major indicators of the rock pore-size distribution. These factors were determined using Mercury porosimetry measurements. Several authors indicated that pore-size distribution has a major role in determining the outcome of a waterflood in a reservoir under capillary pressure dominance. To simulate such fluid flow mechanisms, pore-entry diameter and rock surface area were incorporated in the statistical model.

MODEL-BUILDING PROCESS

Data Collection and Preparation

The types of data considered are divided into two groups: (a) a series of n observations representing single measurements of the same quality characteristic of n similar things, and (b) a series of n observations representing n measurements of the same quality characteristic of one thing.

An example of data of the first type would be 20 observations of residual water saturation from 20 different cores where a description of the data is obtained. The description involves the determination of the mean, median, standard deviation and possible outliers from the data.

The measurement of the thickness of a test core would be an example of the second type of data. If the distribution of the data set (the repeated measurements of the core thickness) is normal, an average of the data set can be generally obtained and is meaningful. If however, the data set contains outliers and is represented by a skewed distribution, a median rather than a mean is more representative of the data set.

In waterflooding and porosimetry measurements, data are classified as data of the first type. However, data obtained from wettability and Klinkenberg air porosity and air permeability measurements are classified as data of the second type.

Reduction of Number of Independent Variables

Once the data has been collected and prepared, the method of upper and lower quartiles, which is comparable to stem-and-leaf plots, was used to identify mild and extreme outliers for each of the independent variables. Additionally, relationships and interaction effects were explored using the independent variables considered in the model.

A first-order regression model relating the ultimate oil recovery (UOR) to all independent variables was fitted. It is presented in the following form:

$$UOR = 0.362 + 0.005\ SA - 0.0263\ d - 0.000064\ \tau - 0.923\ \phi + 0.000027\ k$$
$$- 0.0183\ L + 0.375\ WI - 1.30\ S_{or} + 0.632\ S_{oi}$$

$R^2 = 94.4\%$
$s = 0.00961$
$F = 18.65$
$R^2_N = 98.3\%$

The normal probability plot of the residuals for the full model is presented in Figure 1. Normal probability plots are used to test the residuals normality or departure from normality, identify outliers and test the model's linearity. In addition to the normal probability plot, the residual plot for this particular model is presented in Figure 2. Residual plots test the possibility of error terms correlation and regression function linearity. They are also used to validate the regression model's assumption that the error terms variability is constant. The different coefficient of correlations, R^2_N, for the different tested models between the ordered residuals and their respective values under normality are presented in Table 1; reference to Table 2 supports the conclusion of the error terms being normally distributed.

As shown in Table 3, the correlation matrix with the dependent variable, ultimate oil recovery, was obtained. Tables 1 and 2 and the various residual and normal residual plots all indicate that each of the independent variables is linearly associated with the dependent variable, S_{or} (residual oil saturation) showing the highest degree of association and τ (tortuosity) the lowest. The correlation matrix further shows intercorrelations among the potential independent variables. In particular, SA (surface area) has a high pairwise correlation with L (pore length) and ϕ (porosity) and moderately high pairwise correlation with d (pore-entry diameter) and WI (wettability index). On the basis of these analyses, the dependent variable, ultimate oil recovery, would be represented as a function of the independent variables in linear terms, and not to include any interaction terms. Table 4 shows the pairwise comparison of the different independent variables used in the full-model.

The all-possible-regressions selection procedure calls for a consideration of all possible regression models involving the potential x variables and identifying a few "good" subsets according to some criterion. In most circumstances, it would be impossible to make a detailed examination of all possible regression models. For instance, when there are 8 independent variables in the pool of variables as in the case of this study, there would be $2^8 = 256$ possible regression models. Since the pool of potential x variables is high, this study will concentrate on a few of the possible regression models. According to a different set criteria, this number consists of 40 subsets. These criteria are : R^2_p, MSE_p and C_p.

R^2_p Criterion:

Before examining the different criteria, a notation needs to be developed in which the number of potential x variables in the pool would be denoted by p-1. Additionally, all regression models are assumed to contain an intercept β_o. Hence, the regression function containing all potential x variables contains P parameters, and the function with no x variables contains one parameter (β_o). The number of x variables in a subset will be denoted by p-1, as always, so that there are p parameters in the regression function for this subset of x variables. Therefore, it follows that:

$$1 \leq p \leq P$$

The all-possible-regressions approach assumes that the number of observations exceeds the maximum number of potential parameters: $n > P$. The R^2_p criterion calls for an examination of the coefficient of multiple determination, R^2. The number of parameters in the regression model is shown as a subscript of R^2. Therefore, R^2_p indicates that there are p parameters, or p-1 predictor variables in the regression function on which R^2_p is based.

Since:

$$R^2_p = \frac{SSR_p}{SSTO} = 1 - \frac{SSE_p}{SSTO}$$

and the denominator is constant for all possible regressions, R^2_p varies inversely with the error sums of squares SSE_p. But we know that SSE_p can never increase as additional x variables are included in the model. Therefore, R^2_p will be a maximum when all p-1 potential x variables are included in the regression model. The reason for using the R^2_p criterion with the all-possible-regressions approach, therefore cannot be to maximize R^2_p. Rather, the intent is to find the point where adding more x

variables is not worthwhile because it leads to a very small increase in R^2_p. The R^2_p values as a function of P, the number of parameters, are plotted in Figure 3. The maximum R^2_p value for the possible subsets of p-1 predictor variables, denoted by max (R^2_p), appears at the top of the graph for each p. These points are connected by dashed lines to show the impact of adding additional x variables. Figure 3 makes it clear that little increase in max (R^2_p) takes place after 6 variables are included in the model. Hence, the use of subset (SA, d, τ, WI, S_{or}, S_{oi}) in the regression model appears to be reasonable according to the R^2_p criterion. Note that variables ϕ, porosity, and k, permeability, which correlates most highly with the independent variables, are not in the model of P = 7, indicating that SA, d, τ, WI, S_{or}, S_{oi} contained much of the information presented by ϕ, porosity, and k, permeability.

C_p criterion:

This subset is concerned with the total mean squared error of the n fitted values for each subset regression model. The mean squared error concept involves a bias component and a random error component. The mean squared error pertains to the fitted values $\hat{Y}_i$ for the regression model employed. The bias component for the ith fitted value is:

$$E(\hat{Y}_i) - \mu_i$$

where $E(\hat{Y}_i)$ is the expectation of the ith fitted value for the given regression model and μ_i is the true mean response. The random error component for $\hat{Y}_i$ is simply $\sigma^2(\hat{Y}_i)$, its variance. The model which includes all p-1 potential x variables is assumed to have been carefully chosen so that $MSE(X_1,...,X_{p-1})$ is an unbiased estimator of σ^2. It can be shown that

$$Cp = \frac{SSE_p}{MSE(X_1,..., X_{p-1})} - (n-2p)$$

where SSE_p is the error sum of squares for the fitted subset regression model with p parameters. When there is no bias in the regression model with p-1 predictor variables so that $E\{\hat{Y}_i\} = \mu_i$, the expected value of C_p is approximately p:

$$E\{C_p \mid E\{\hat{Y}_i\}$$

Therefore, when the C_p values for all possible regression models are plotted against, those models with little bias will tend to fall near the line $C_p = p$. Models with substantial bias will tend to fall considerably above this line. C_p values below the line $C_p = p$ are interpreted as showing no bias; that is, they are below the line due to sampling error. In using the C_p criterion, one seeks to identify subsets of X variables for which (1) the C_p value is small and (2) the C_p value is near p. Sets of x variables with small C_p values have a small total mean squared error, and when the C_p value is also near p, the bias of the regression model is small. The C_p values for the selected models are plotted as a function of P, the number of parameters, in Figure 4. As shown in Figure 5, plotting C_p values against R^2_p values suggested that subset (SA, d, τ, WI, S_{or}, S_{oi}) is a better choice than the full model.

Model Refinement and Selection

After successfully reducing the number of independent variables, variables such as SA, d, τ, WI, S_{or} and S_{oi} are known to be essential. The nonstandardized multiple regression model presented the difficulty that the ordinarily regression coefficients can not be compared because of differences in units involved. To eliminate the problem of lack of comparability in regression coefficients a correlation

transformation was used. The use of correlation transformation helps with controlling roundoff errors and makes the units in the regression coefficients comparable.

The correlation transformation is a simple modification of the usual standardization of a variable. Standardizing a variable involves taking the difference between each observation and the mean of all observations and then expressing the differences in units of the standard deviation of the observations. Therefore, the usual standardizations of the dependent variable Y and the independent variables $X_1,...,X_{p-1}$ are as follows:

$$\frac{Y_i - \bar{Y}}{s_Y}$$

$$\frac{X_{ik} - \bar{X}_k}{s_k} \qquad (k = 1,...,p-1)$$

Where $\bar{Y}$ and $\bar{X}_k$ are the respective means of Y and X_k, and s_Y and s_k are the respective standard deviations defined as follows:

$$s_Y = \sqrt{\sum_{i=1}^{n} \frac{(Y_i - Y)^2}{(n-1)}}$$

$$s_k = \sqrt{\sum_{i=1}^{n} \frac{(X_{ik} - X_k)^2}{(n-1)}} \qquad (k=1,...,p-1)$$

The correlation transformation uses the following function of the standardized variables in:

$$Y'_i = \frac{1}{\sqrt{n-1}}\left(\frac{Y_i - \bar{Y}}{s_Y}\right)$$

$$X'_{ik} = \frac{1}{\sqrt{n-1}}\left(\frac{X_{ik} - \bar{Y}_k}{s_k}\right) \qquad (k=1,...,p-1)$$

Standardized Regression Model

The regression model with the transformed variables Y′ and X'_k as defined by the correlation transformation is called a standardized regression model and is as follows:

$$Y'_i = \beta'_1 X'_{i1} + \cdots + \beta'_{p-1} X'_{i,p-1} + \varepsilon'_i$$

The reason why there is no intercept parameter in the standardized regression model is that the least squares calculations always would lead to an estimated intercept term of zero if an intercept parameter were present in the model.

It is easy to show that the new parameters $\beta'_1,\ldots, \beta'_{p-1}$ and the original parameters $\beta_o, \beta_1,\ldots, \beta_{p-1}$ in the ordinary multiple regression model are related as follows:

$$\beta_k = (\frac{S_Y}{S_k})\beta'_k \qquad (k=1,\ldots,p-1)$$

$$\beta_0 = \overline{Y} - \beta_1\overline{X}_1 - \cdots - \beta_{p-1}\overline{X}_{p-1}$$

Therefore, the new regression coefficients β'_k and the original regression coefficients β_k, (k=1,...,p-1), are related by simple scaling factors involving ratios of the standard deviations.

At this stage, the model relating the dependent variable ultimate oil recovery (UOR) to the previously mentioned independent variables is presented as follows:

$$UOR = 0.0052 + 0.252\ SA - 0.167\ d - 0.454\ \tau + 0.464\ WI - 1.74\ S_{or} + 1.08\ S_{oi}$$

$R^2 = 92.8\%$
$s = 0.0754$
$F = 27.92$
$R^2_N = 98.4\%$

The residual and normal residual plots for this particular model are presented in Figures 6 and 7, respectively. Reference to Figures 3, 4 and 5 and to Table 1 lead to the conclusion that this model is the preferred model. This model is preferred over other models since it uses essential variables, has a high coefficient of multiple determination ($R^2 = 92.8\%$), uses fewer variables (6), has a low standard deviation (s=0.0754), and its first-order classification stands since the error terms are strongly normal ($R^2_N = 98.4\%$). Reducing the selected model resulted in higher values of C_p which lead to the conclusion that the bias in these models is large as shown in Table 1. Among the reduced models, we selected the following:

$$UOR = 0.0034 + 0.451\ SA - 0.166\ d - 0.412\ \tau + 0.631\ WI - 0.636\ S_{or}$$

$R^2 = 83.0\%$
$s = 0.1116$
$F = 13.70$
$R^2_N = 96.7\%$

The residual and normal residual plots for this particular model are presented in Figures 8 and 9, respectively. Reduction of the chosen model resulted in higher standard error (s = 0.1116), lower coefficient of multiple determination ($R^2 = 83.0\%$), and a larger ($C_p = 22.183$) indicating a higher bias in the model. The residuals were less normal ($R^2_N = 96.7\%$) leading to the conclusion that the first-order model classification is less powerful.

Model Validation

Two models out of the literature are selected to test and validate the model selected. One of these models was presented by Donaldson, Thomas and Lorenz (19). The statistical model related oil

recovery to wettability, permeability, porosity, oil viscosity and initial oil saturation.

$$UOR = -0.007 - 1.12\ \phi + 0.470\ k + 0.410\ WI - 0.369\ S_{oi}$$

$R^2 = 72.8\%$
$s = 0.1380$
$F = 8.04$
$R^2_N = 94.3\%$

The other tested model developed by Arnold and Crawford (20) is an empirical equation relating oil and rock properties to waterflooding recoveries. The empirical equation correlates oil recovery to porosity, permeability and initial oil saturation. The model was used to test and validate our data.

$$UOR = -8.52 + 0.00224\ k - 12.1\ S_{oi} + 4.7 \times 10^{-7}\ k^2 + 1.24\ S_{oi}^2 + 63.0\ \phi\ S_{oi}$$

$R^2 = 77.1\%$
$s = 0.0177$
$F = 5.76$
$R^2_N = 97.2\%$

The additional variables incorporated in our model, surface area, pore-entry diameter, and tortuosity, which best describe rock skeletal properties, were used to simulate fluid flow mechanisms in a porous medium where capillary forces are dominant. Their addition improved drastically the summation of squares for regression and the model prediction capabilities by lowering the margin of bias and random errors.

CONCLUSIONS

The experimental work on which the correlations presented here is based, dealt with water-wet media under laboratory conditions. It was shown that oil recovery by waterflooding, in a porous medium under capillary forces dominance, can be better estimated if microscopic rock skeletal properties such as surface area, pore-entry diameter and tortuosity can be incorporated into an empirical equation.

- The standardized regression model selected, although in a reduced form, predicted oil recovery by waterflooding with an a standard deviation of 7 per cent. The fact that in this model C_p is slightly lower than P is the result of random variation in the C_p estimate. In addition, the reduced model was standardized due to the lack of comparability in regression coefficients. The full model (not in a standardized form) which involves 10 parameters predicted oil recovery with a standard deviation of 1 per cent.

- Thirty nine other equations were developed. Some of these models are associated with high standard deviations, low coefficients of multiple determinations or substantial bias. Very few models are associated with C_p values tending to fall below the line $C_p = p$. These models are interpreted to show no bias; that is, they are below the line due to sampling error.

ACKNOWLEDGMENTS

The authors wish to acknowledge the financial support of the U.S. Department of Energy to the Pennsylvania State University through Contract No. DE-AC22-89BC14477.

LITERATURE CITED

1. Pickell, J.J., B.F. Swanson and W.B. Hickman, *Society of Petroleum Engineers Journal*, **6** 1, 55-61 (March, 1966).

2. Purcell, W.R., *Petroleum Transactions, American Institute of Mining, Metallurgical, and Petroleum Engineers Inc.*, **186**, 39-48 (1949).

3. Chatzis, I., N. Morrow and H.T. Lim, *Petroleum Transactions, American Institute of Mining, Metallurgical, and Petroleum Engineers Inc.*, 312 (April, 1983).

4. Kimbler, O.K. and B.H. Caudle, *Oil and Gas Journal*, **55**, 85-88 (1957).

5. Engelberts, W.P. and F.M. Perkins, Jr., *Proc., Third World Congress*, Section II.

6. Craig, F.F., "The Reservoir Engineering Aspects of Waterflooding," Society of Petroleum Engineers Monograph Series 3, 3 (1971).

7. Watson, R.W. and F.H. Boukadi, *Society of Core Analysts*, Conference paper 9007, 36p (August, 1990).

8. Wardlaw, N.C. and R.P. Taylor, *Bulletin of Canadian Petroleum Geology*, **24**, 225-62 (June, 1976).

9. Chatzis, I. and F.A.L. Dullien, *Powder Technology*, **29**, 117-25 (1981).

10. Wyman, R.E., *Bulletin of Canadian Petroleum Geology*, **25**, 233-70 (May, 1977).

11. Willhite, G.P., WATERFLOODING, *SPE Textbook Series*, **3**, 36 (1986).

12. Amthor, J.E., D.C. Kopaska-Merkel and G.M. Friedman, *Carbonates and Evaporites*, **3** 1, 33-52 (1988).

13. Reverberi, G., G. Feraiolo and A. Peloso, *Ann. Chim.*, (Italy), **1552**, 56 (1966).

14. Lowell, S. and J.E. Shields, *Journal of Colloid Interface Science*, **80**, 192 (1980).

15. Wardlaw, N.C., *Bulletin of Canadian Petroleum technology*, **21** 3, 7p (May-June, 1982).

16. Roof, J.G., *Society of Petroleum Engineers Journal*, 85-90 (March, 1970).

17. Erle, M.A., D.C. Dyson, and N.R. Morrow, *American Institute of Chemical Engineers Journal*, 17, 115-21 (1971).

18. Mohanty, K.K., H.T. Davis and L.E. Scriven, *Society of Petroleum Engineers Journal*, paper 9406, (Sept. 21-24, 1980).

19. Donaldson, E.C., R.D. Thomas and P.B. Lorenz, *Society of Petroleum Engineers Journal*, SPE paper 2338, (March 1969).

20. Arnold, M.D. and P.B. Crawford, *Society of Petroleum Engineers of AIME*, SPE paper number 847, microfiche, pp. 43-52.

Table 1: R_p^2, MSE_p, C_p and R_N^2 Values for the Investigated Regression Models

Variables	p	df	SSE_p	R^2_p	MSE_p	C_p	R^2_N
S_{wi}	2	18	0.0112241	31.6	0.0006236	105.604	0.983
S_{or}	2	18	0.0067652	58.8	0.0003758	57.296	0.973
WI	2	18	0.0150823	8.1	0.0008379	147.405	0.978
L	2	18	0.0152882	6.9	0.0008493	149.636	0.924
K	2	18	0.0142500	13.2	0.0007917	138.388	0.930
ϕ	2	18	0.0130872	20.3	0.0007271	125.790	0.941
τ	2	18	0.0157821	3.9	0.0008768	154.987	0.957
D	2	18	0.0141766	13.7	0.0007876	137.593	0.927
SA	2	18	0.0132774	19.1	0.0007376	127.850	0.941
S_{or}, S_{wi}	3	17	0.0035314	78.5	0.0002077	24.260	0.783
τ, S_{or}	3	17	0.0067608	58.8	0.0003977	59.248	0.973
τ, S_{oi}	3	17	0.0109953	33.0	0.0006468	105.126	0.984
τ, S_{or}, S_{oi}	4	16	0.0029848	81.8	0.0001865	20.338	0.783
τ, WI, S_{or}	4	16	0.0064027	61.0	0.0004002	57.368	0.987
τ, WI, S_{oi}	4	16	0.0010540	35.8	0.0006588	102.198	0.990
WI, S_{or}, S_{oi}	4	16	0.0035299	78.5	0.0002206	26.244	0.783
τ, WI, S_{or}, S_{oi}	5	15	0.0026293	84.0	0.0001753	18.486	0.876
SA, d, τ, WI, S_{or}	6	14	0.0027859	83.0	0.0001990	22.183	0.967
SA, d, τ, WI, S_{oi}	6	14	0.0047629	71.0	0.0003402	43.602	0.981
SA, d, τ, S_{or}, S_{oi}	6	14	0.0020582	87.5	0.0001470	14.299	0.957
SA, d, WI, S_{or}, S_{oi}	6	14	0.0020506	84.7	0.0001790	19.148	0.943
SA, τ, WI, S_{or}, S_{oi}	6	14	0.0014184	91.4	0.0001013	7.367	0.988
d, τ, WI, S_{or}, S_{oi}	6	14	0.0014756	91.0	0.0001054	7.987	0.987
SA, d, τ, WI, S_{or}, S_{oi}	7	13	0.0011822	92.8	0.0000909	6.808	0.984
SA, d, τ, L, WI, S_{or}	7	13	0.0019949	87.9	0.0001535	15.613	0.978
SA, d, τ, L, WI, S_{oi}	7	13	0.0035260	78.8	0.0002712	32.201	0.983
SA, d, τ, L, S_{or}, S_{oi}	7	13	0.0018647	88.6	0.0001434	14.203	0.961
SA, d, L, WI, S_{or}, S_{oi}	7	13	0.001924	88.4	0.0001471	14.719	0.971
SA, τ , L, WI, S_{or}, S_{oi}	7	13	0.0014135	91.4	0.0001087	9.314	0.975
d, τ , L, WI, S_{or}, S_{oi}	7	13	0.0014753	91.0	0.0001135	9.984	0.987
SA, d, τ , L, WI, S_{or}, S_{oi}	8	12	0.0010678	93.5	0.0000890	7.569	0.993
SA, d, τ, ϕ, K, L, WI, S_{or}	9	11	0.0014350	91.3	0.0001305	13.547	0.985
SA, d, τ, ϕ, K, L, WI, S_{oi}	9	11	0.0028059	82.9	0.0002551	28.400	0.970
SA, d, τ, ϕ, K, L, S_{or}, S_{oi}	9	11	0.0012183	92.6	0.0001108	11.199	0.965
SA, d, τ, ϕ, K, WI, S_{or}, S_{oi}	9	11	0.0010853	93.4	0.0000987	9.758	0.995
SA, d, τ, ϕ, L, WI, S_{or}, S_{oi}	9	11	0.0009537	94.2	0.0000867	8.333	0.992
SA, d, ϕ , K, L, WI, S_{or}, S_{oi}	9	11	0.0013351	91.9	0.0001214	12.465	0.984
SA, τ, ϕ, K, L, WI, S_{or}, S_{oi}	9	11	0.0013160	92.0	0.0001196	12.258	0.983
d, τ, ϕ, K, L, WI, S_{or}, S_{oi}	9	11	0.0009233	94.4	0.0000839	8.000	0.983
SA, d, τ, ϕ, K, L, WI, S_{or}, S_{oi}	10	10	0.0009231	94.4	0.0000923	10.00	0.983

Table 2: Table of Alpha Critical Values

	α				α		
N	.10	.05	.01	N	.10	.05	.01
4	.8951	.8734	.8318	30	.9707	.9639	.9490
5	.9033	.8804	.8320	40	.9767	.9715	.9597
10	.9347	.9180	.8804	50	.9807	.9764	.9664
15	.9506	.9383	.9110	60	.9835	.9799	.9710
20	.9600	.9503	.9290	75	.9865	.9835	.9757
25	.9662	.9582	.9408				

Table 3: Correlation Matrix for the Full-Model

	SA	d	τ	ϕ	k	L	WI	S_{or}	S_{wi}	UOR
d	-0.609									
τ	-0.027	-0.052								
ϕ	-0.688	0.361	-0.192							
k	-0.628	0.517	0.075	0.138						
L	0.753	-0.771	0.151	-0.518	-0.476					
WI	-0.418	0.081	0.705	0.054	0.350	-0.196				
S_{or}	-0.222	0.009	-0.277	0.808	-0.456	-0.146	-0.250			
S_{wi}	0.108	0.093	0.143	-0.658	0.634	0.103	0.153	-0.937		
UOR	0.437	-0.370	0.197	-0.806	-0.011	0.262	0.285	-0.767	0.513	1.000

Table 4: Pairwise Comparison of the Different Independent Variables Used in the Model

Variables	p	df	SSE_p	R^2_p	MSE_p	C_p
SA, d	2	18	0.0108006	37.1	0.006000	101.016
τ, SA	2	18	375949	0.1	20886	-
τ, d	2	18	375192	0.3	20844	-
τ, ϕ	2	18	0.0043970	0.0	0.002443	31.638
ϕ, d	2	18	0.0029460	33.0	0.0001630	15.918
ϕ, SA	2	18	0.0005090	88.4	0.0000283	-10.485
k, τ	2	18	671145	0.3	37286	-
k, d	2	18	495325	26.4	27518	-
k, SA	2	18	116155	82.7	6453	-
L, k	2	18	1.5626	49.5	0.0868	-
L, ϕ	2	18	1.4719	52.5	0.0818	-
L, τ	2	18	3.0259	2.3	0.1681	-
L, d	2	18	1.2544	59.5	0.0897	-
L, SA	2	18	1.3386	56.8	0.0744	-
WI, L	2	18	0.01115	3.9	0.0006194	104.802
SA, S_{wi}	2	18	0.025288	1.2	0.501405	257.976
d, S_{wi}	2	18	0.025366	0.9	0.001409	258.821
τ, S_{wi}	2	18	0.025067	2.0	0.001393	255.582
ϕ, S_{wi}	2	18	0.025584	0.0	0.001421	261.183
k, S_{wi}	2	18	0.025542	0.2	0.001419	260.728
L, S_{wi}	2	18	0.025315	1.1	0.001406	258.269
WI, S_{wi}	2	18	0.024986	2.3	0.001388	254.704
S_{wi}, S_{or}	2	18	0.003146	87.7	0.000125	18.084
d, S_{or}	2	18	0.021791	0.0	0.001211	220.089
τ, S_{or}	2	18	0.020115	7.7	0.001117	201.931
ϕ, S_{or}	2	18	0.021352	2.0	0.001186	215.333
k, S_{or}	2	18	0.021517	1.3	0.001195	217.120
L, S_{or}	2	18	0.021328	2.1	0.001185	215.072
SA, S_{or}	2	18	0.020717	4.9	0.001151	208.453
WI, S_{or}	2	18	0.020430	6.3	0.001135	205.343
WI, SA	2	18	0.00905665	17.5	0.0005315	87.646
WI, d	2	18	0.0115206	0.7	0.0006400	108.817
WI, τ	2	18	0.0058348	49.4	0.0003242	47.216
WI, ϕ	2	18	0.0105598	8.9	0.0005867	98.407
WI, k	2	18	0.0102121	11.9	0.0005673	94.640

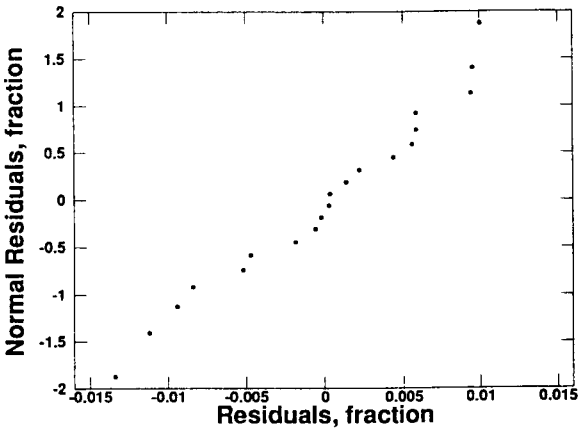

Fig. 1: Normal Probability Plot (Full-Model)

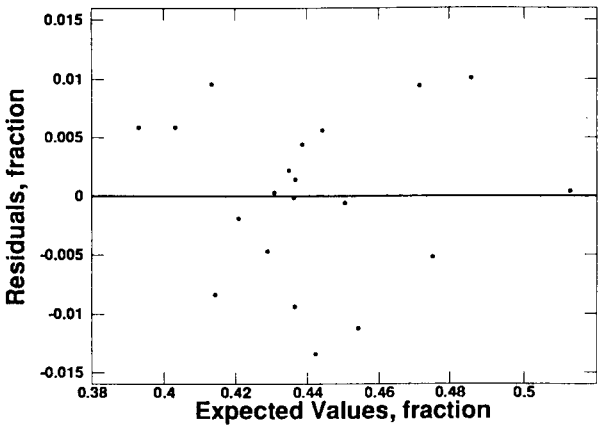

Fig. 2: Residual Plot vs Expected Values (Full-Model)

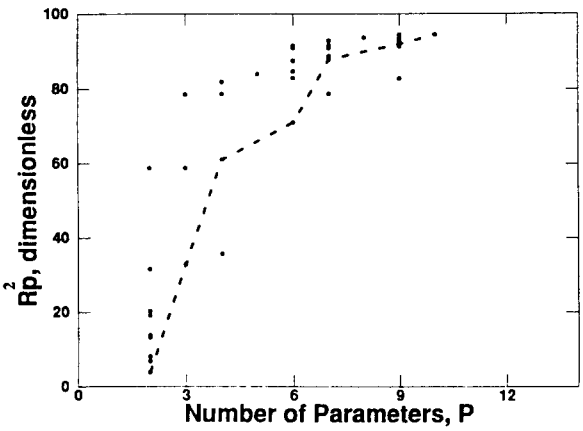

Fig. 3: R_p^2 vs Number of Parameters Plot

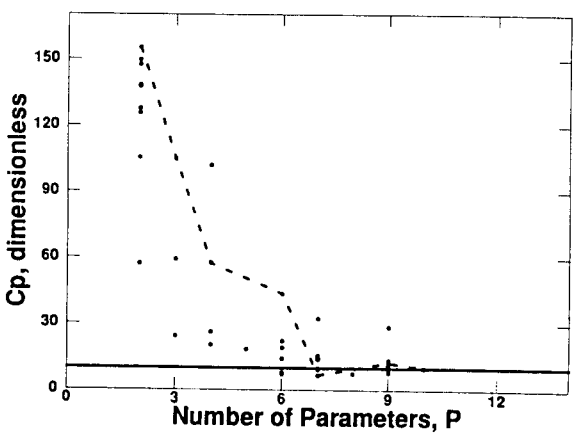

Fig. 4: C_p vs Number of Parameters Plot

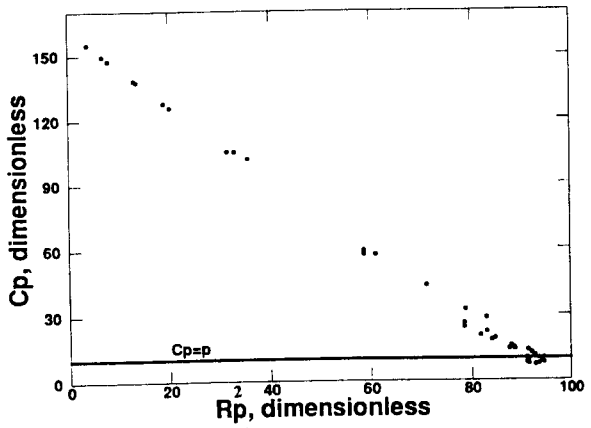

Fig. 5: C_p vs R_p^2 Plot

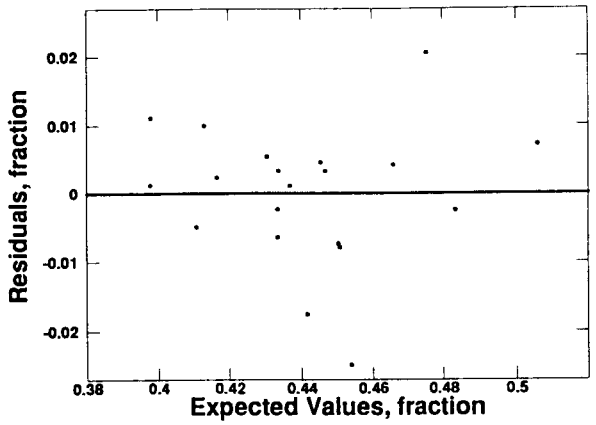

Fig. 6: Residual Plot vs Expected Values (Reduced-Model)

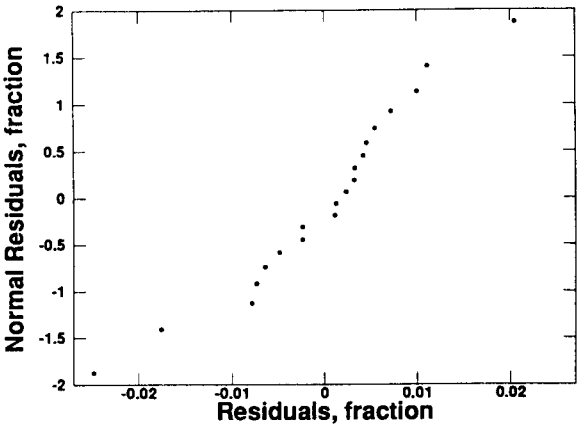

Fig. 7: Normal Probability Plot (Reduced-Model)

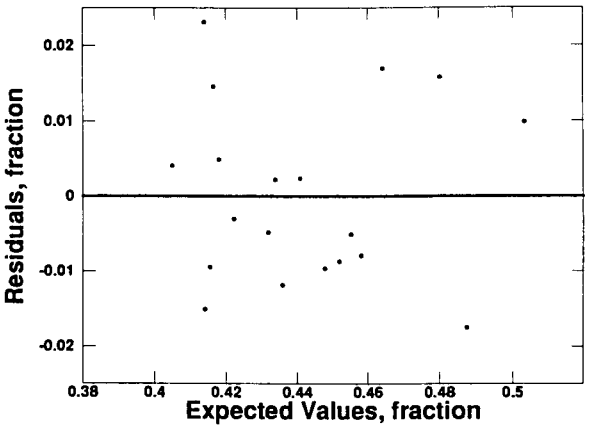

Fig. 8: Residual Plot vs Expected Values (Further Reduced-Model)

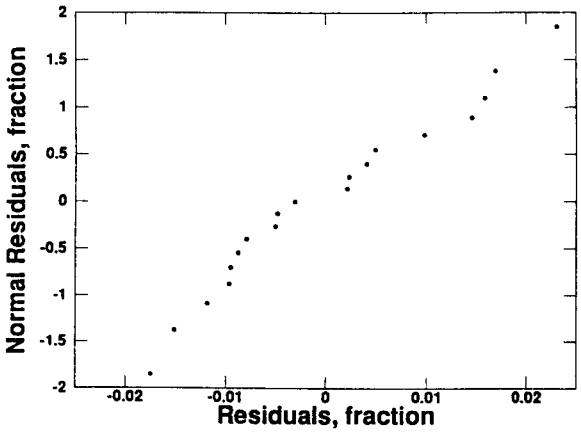

Fig. 9: Normal Probability Plot (Further Reduced-Model)